Nuclear Instruments and Methods 193 (1982) 557–561
North-Holland Publishing Company

IMPROVEMENT OF TIME RESULUTION OF COAXIAL Ge(Li) DETECTORS BY TIME WALK CORRECTION

J. KASAGI *, H. OHNUMA
Department of Physics, Tokyo Institute of Technology, Meguro-ku, Tokyo, Japan

and

N. OHYAMA
Image Science and Engineering Laboratory, Tokyo Institute of Technology, Nagatsuta, Midori-ku, Yokohama, Japan

Received 29 January 1981 and in revised form 24 July 1981

A technique to correct the time walk due to the rise-time change has been developed in order to improve the time resolution of coaxial Ge(Li) detectors. Typical time resolutions (fwhm) of 2.0 ns for 1332 keV gamma rays and 3.4 ns for 511 keV gamma rays have been obtained for a 60 cm^3 coaxial Ge(Li) detector. It is emphasized that the improvement can be achieved without any loss of efficiency.

1. Introduction

It is well known that the charge collection time of a coaxial Ge(Li) detector is not constant but depends on the details of the interactions within the crystal producing a particular pulse. This variation is reflected in the pulse-shape change at preamplifier and fast amplifier outputs. Timing discriminators introduced to improve the time resolution [1,2] usually compensate the time walk due to the pulse-height change, but the time walk due to the pulse-shape change is poorly compensated by these discriminators. The time resolution of large coaxial Ge(Li) detectors, therefore, is mainly limited by this variation in pulse shapes.

Much improved time resolution of coaxial Ge(Li) detectors has been obtained by White and McDonald [3], using a pulse-shape discrimination technique with a dual constant fraction discriminator. Their result shows the possibility of improving the time resolution by selecting pulses with a certain rise-time. However, the detection efficiency is inevitably reduced to about 60%.

We have developed a method to improve the time resolution of large coaxial Ge(Li) detectors. The method presented here is to correct the time walk using the correlation between the rise-time and the timing output. It is emphasized that a much improved time resolution can be obtained without any loss in efficiency.

2. Pulse shape considerations

The pulse used for the timing system input depends not only on the manner in which electric charge is collected by the detector electrodes but also depends on the response of an amplifying chain between the detector output and the timing system input. A preamplifier, a timing filter amplifier (TFA) and a constant fraction discriminator (CFD) are used in a conventional setup. Therefore we consider here the pulse shape of the TFA output, assuming that the charge produced by the interaction of a gamma ray with the detector is localized to a point.

Calculated pulse shapes at the TFA output are shown in fig. 1 for different interacting positions. Here R is the radius at which the gamma ray is absorbed. The details of the calculation are described in Appendix. As shown in fig. 1, the rise-time of the TFA output pulse is strongly affected by R. The peak

* Present address: Cyclotron Laboratory, Michigan State University, East Lansing, MI 48824, U.S.A.

0029-554X/82/0000–0000/$02.75

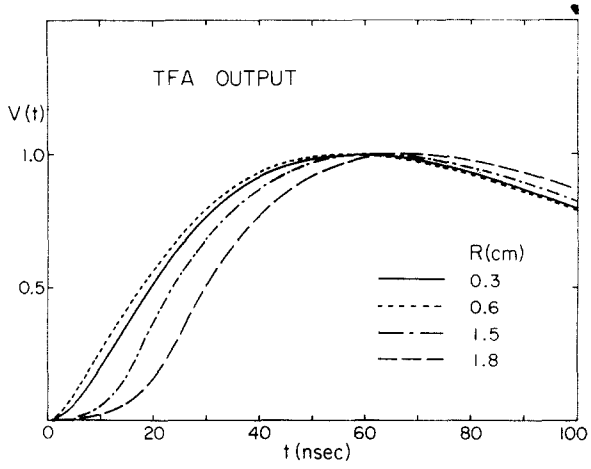

Fig. 1. Calculated pulse shape of the TFA output for various interaction positions (R). Details of the calculation and the parameter are described in the appendix.

positions of the pulses change by about 20 ns. In fig. 2 are shown the pulses synthesized according to the amplitude and rise-time compensation (ARC) method [1]. The zero cross-time of the synthesized pulse corresponds to the CFD output. The time walk of the CFD output is then more than 10 ns as can be seen in fig. 2. This effect leads to the poor time resolution of

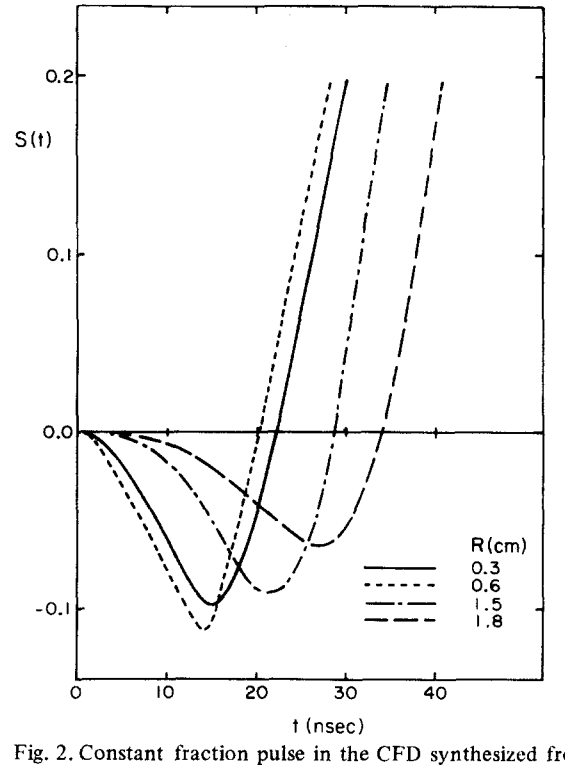

Fig. 2. Constant fraction pulse in the CFD synthesized from the TFA output pulse with 13 ns delay time and 0.3 fraction.

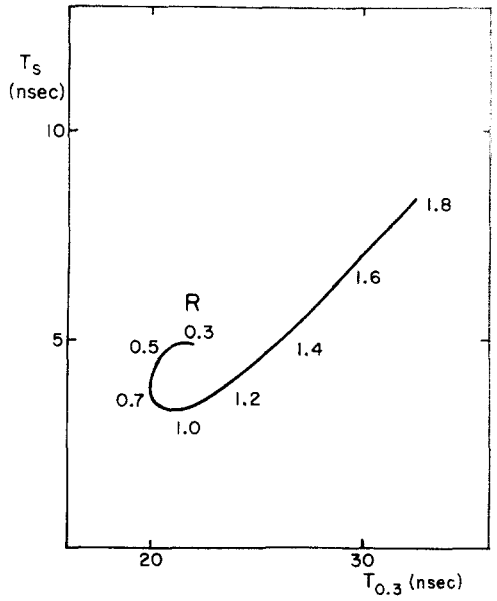

Fig. 3. Calculated correlation between the timing output of $F = 0.3$ CFD ($T_{0.3}$) and the time difference of that from the $F = 0.1$ CFD output (T_S). R indicates the interacting position in cm.

the coaxial Ge(Li) detectors. The time walk due to the pulse-shape change cannot be much improved by changing the fraction.

In fig. 3 the plot of the time difference (T_S) between the outputs of CFDs with the fraction of 0.1 ($F = 0.1$) and of 0.3 ($F = 0.3$) against the $F = 0.3$ output ($T_{0.3}$). The value of $T_{0.3}$ increases with increasing T_S for $T_{0.3} > 21$ ns. The calculated relation below $T_{0.3} \simeq 25$ ns is not simple. Two values of $T_{0.3}$ correspond to one value of T_S. However, this complexity would not deteriorate the time resolution because the effeciency becomes smaller with smaller R. Therefore, the time resolution of the coaxial detector is expected to be improved by the correction of the $T_{0.3}$ value determined by the relation between the $T_{0.3}$ and T_S. The relation must be deduced experimentally because the charge carrier generation in different parts of the detector volume contributes to the final pulse formation.

3. Experimental details and results

The time resolution of 60 cm^3 and 32 cm^3 coaxial Ge(Li) detectors were measured using the ^{22}Na and ^{60}Co sources. A block diagram of the electronic arrangement is shown in fig. 4. A timing coicidence

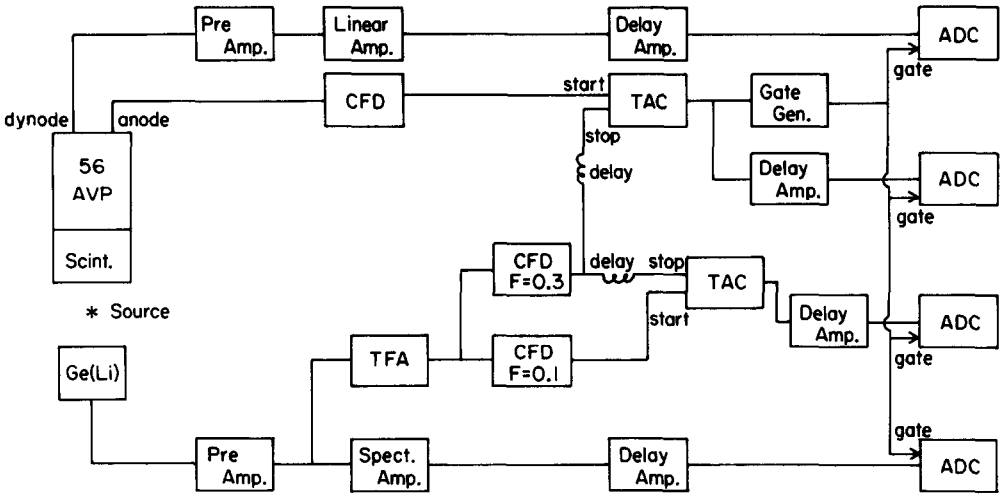

Fig. 4. Block diagram of the electronics used in the experiments

was obtained between the Ge(Li) detector and a plastic scintillator counter with a 56AVP photomultiplier. The time resolution of the latter detector was about 0.5 ns, which contributes negligibly (~3%) when combined in quadrature with the Ge(Li) time resolution. The outputs of the $F = 0.1$ and $F = 0.3$ CFDs were used as start and stop pulses of a time-to-amplitude-converter (TAC) the output of which was used for pulse-shape information as mentioned in the previous section (hereafter this TAC will be called STAC). The output of the $F = 0.3$ CFD was also used as a stop pulse of another TAC the output of which corresponds to the timing information of the Ge(Li) detector. Energy pulses from the Ge(Li) detector and the plastic counter as well as the outputs of the TACs were fed to ADCs. The digitized information was written on magnetic tape through a computer for the off-line analysis.

The correlation between the STAC output and the centroid of the TAC peak is shown in fig. 5. The main feature of the correlation is the fact that the centroid of the peak increases monotonously as the STAC channel increases and that the shift of the centroid becomes very small with STAC beyond about 90 ch. The resolution of each peak does not change very much. The obtained best resolution for the 1332 keV gamma ray is 1.9 ns and the worst one is about 2.6 ns. This observation does not contradict that of ref. 3. If the TAC signals are sorted by setting a larger window on STAC, the TAC spectrum obtained would display a worse time resolution. Therefore, the present data clearly demonstrate that the main cause of the time resolution deterioration is the change of the timing output due to the shape change. The obtained correlation for the 1332 keV gamma ray is slightly different from that of the 511 keV gamma

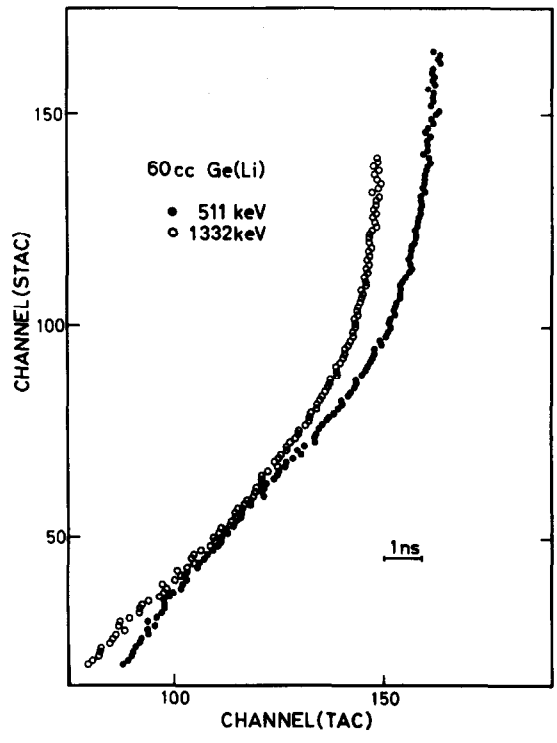

Fig. 5. Plot of the centroid channel of the time spectra as a function of the STAC output for 511 keV and 1332 keV gamma rays measured by a 60 cm^3 Ge(Li) detector.

ray. This difference may be due to the difference in the multiple scattering effect.

The least-squares fit was made for each curve with the fitting function $C(\mathrm{ch_s}) = \Sigma a_n \cdot \mathrm{ch_s}^n$. Here $C(\mathrm{ch_s})$ is the centroid of the TAC peak, $\mathrm{ch_s}$ is the channel number of the STAC and the a_n values are the coefficients to be determined by the fitting. The TAC outputs are shifted by using the obtained fitting functions in such a way that the TAC–STAC correlation becomes a straight vertical line. In this correction, performed in an event-by-event mode, the final channel number of the TAC is calculated from the STAC channel number as $N_c = N_u + C_0 - C(\mathrm{ch_s})$, where N_c and N_u are the corrected and uncorrected TAC channel number, respectively, and C_0 is a given constant channel number at which the centroid of the final TAC spectrum is expected.

The final TAC spectra are shown in fig. 6 along with the uncorrected spectra for the 60 cm^3 Ge(Li) detector. The significance of this correction method can be clearly seen in these spectra. The time spectra without correction have the tail on the slopes. On the other hand the line shapes of the corrected spectra are symmetrical and have better resolutions.

The time resolutions obtained of the 60 cm^3 and 32 cm^3 Ge(Li) detectors are listed in table 1. The figures in parentheses are those without correction. The time resolution has been improved by about 20% at fwhm and by about 50% at fw(1/10)m and fw(1/100)m. It should be noticed that these improvements can be obtained without a loss in efficiency. The slopes of the tail of the time spectra correspond to the decay time of 0.55 ns for 1332 keV gamma ray and 0.75 ns for 511 keV gamma ray. The time resolution is mainly determined by noise level, not by geometrical structure, because the resolution deterioration due to the pulse shape change is already removed. Therefore, this time walk correction technique makes it possible to measure lifetime of less than a few ns using the large coaxial Ge(Li) detector. When we deal a complicated gamma-ray spectrum in an actual experiment, all we have to do is to determine the coefficients a_n at several energies and store them in a computer beforehand.

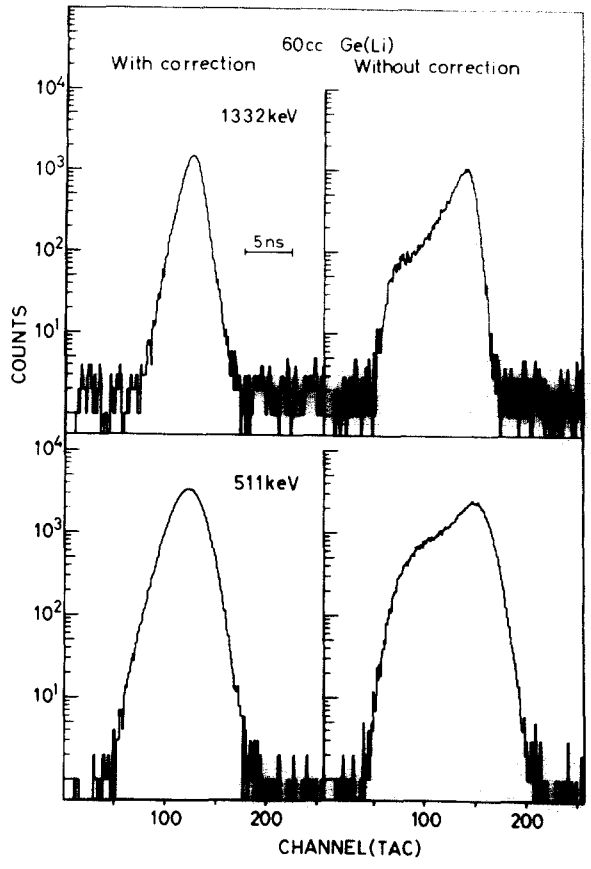

Fig. 6. Corrected and non-corrected TAC spectra of a 60 cm^3 coaxial Ge(Li) detector for 1332 keV and 511 keV gamma rays.

Table 1
Time resolution of Ge(Li) detectors

Detector	E (Mev)	fwhm (ns)	fw(1/10)m (ns)	fw(1/100)m (ns)
60 cm^3 Ge(Li)	1.332	2.0 (2.4)	4.3 (7.0)	7.5 (11.7)
	0.511	3.4 (4.1)	6.7 (11.7)	10.3 (14.6)
32 cm^3 Ge(Li)	1.332	1.8 (2.9)	4.2 (6.7)	6.5 (11.9)
	0.511	3.1 (3.5)	6.4 (11.7)	9.6 (14.6)

Appendix

The ouput pulse shape of the TFA is calculated by using a simplified circuit model given in ref. 4. In the following calculation, the preamplifier is considered as an ideal integrator. Then, the output pulse of the TFA is given as

$$E(p) \propto \frac{1}{pC} \frac{p}{(p + 1/\tau_d)(p + 1/\tau_i)} I_d(p), \quad (1)$$

where $I_d(p)$ is the Laplace transform of the current sources of the detector, C is the effective capacitance of the preamplifier, and τ_d and τ_i are the differential and integral time constants of the TFA.

In order to obtain the analytical expression of the inverse transformation of eq. (1), the following equations are used for the current induced by the hole (I_h) and the electron (I_e) carrier:

$$I_h(t) = K\mu_h \frac{1}{R^2} \left[1 + \left(\frac{1}{a^2} - \frac{1}{R^2}\right) R^2 e^{-1} \frac{t}{T_h} e^{t/T_h}\right],$$

for $t \leqslant T_h$ (2a)

and

$$I_e(t) = K\mu_e \frac{1}{R^2} \left[1 + \left(\frac{1}{b^2} - \frac{1}{R^2}\right) R^2 e \frac{t}{T_e} e^{-t/T_e}\right],$$

for $t \leqslant T_e$ (2b)

where a is the p-core radius, b is the detector radius, R is the radius at which the carrier is created, μ_h and μ_e are the mobility of the hole and electron, K is a constant that depends on the bias voltage (V), T_h and T_e are the charge collection time given by

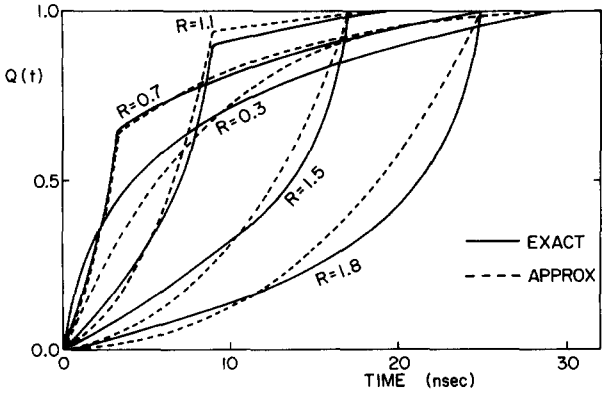

Fig. 7. Charge collection curves of the coaxial detector for various interacting positions (R). The solid lines represent the exact calculations for an ideal double-open-ended coaxial detector and the dotted lines represent calculations from eq. (2).

$$T_h = \frac{\log(b/a)}{2V\mu_h} (R^2 - a^2) \quad (3a)$$

and

$$T_e = \frac{\log(b/a)}{2V\mu_e} (b^2 - R^2). \quad (3b)$$

Fig. 7 shows the charge collection curves as a function of time calculated using eq. (2) along with the exact calculation for an ideal double open-ended coaxial detector [3].

The Laplace transformation of the detector current is then obtained as

$$I_d(p) = \int_0^{T_h} I_h(t) e^{-pt} dt + \int_0^{T_e} I_e(t) e^{-pt} dt$$

$$= K\mu_h \left\{ \frac{1}{R^2} \frac{1}{p} (1 - e^{-pT_h}) + \frac{(1/a^2 - 1/R^2)}{(p - 1/T_h)} \right.$$

$$\times \left[\frac{e^{-1}}{T_h} \frac{1}{(p - 1/T_h)} \right.$$

$$\left. \left. - \left(1 + \frac{1}{T_h} \frac{1}{(p - 1/T_h)}\right) e^{-pT_h} \right] \right\}$$

$$+ K\mu_e \left\{ \frac{1}{R^2} \frac{1}{p} (1 - p^{-pT_e}) + \frac{(1/b^2 - 1/R^2)}{(p + 1/T_e)} \right.$$

$$\times \left. \left[\frac{e}{T_e} \frac{1}{(p + 1/T_e)} - \left(1 + \frac{1}{T_e} \frac{1}{(p + 1/T_e)}\right) e^{-pT_e} \right] \right\}.$$

Inserting eq. (4) into eq. (1) makes it possible to obtain the inverse Laplace transformation analytically. Differentiation and integration in the TFA are used to reduce pile-up at the discriminator input and to reduce high frequency noise, respectively. Therefore, the pulse shape considered in section 2 is calculated with the time constant of $\tau_d = \tau_i = 50$ ns. Other parameters used in the calculation are $a = 0.3$ cm, $b = 1.8$ cm, $V = 2700$ V, $\mu_h = 4.2 \times 10^4$ cm^2 V^{-1} s^{-1} and $\mu_e = 3.6 \times 10^4$ cm^2 V^{-1} s^{-1} [5].

References

[1] R.L. Chase, Rev. Sci. Instr. 39 (1968) 1318; L. Karlsson, Nucl. Instr. and Meth. 106 (1973) 161.
[2] F. Gabriel, H. Koepernik and K. Schops, Nucl. Instr. and Meth. 103 (1972) 501.
[3] D.C. White and W.J. McDonald, Nucl. Instr. and Meth. 115 (1974) 1.
[4] M.O. Bedwell and T.J. Paulus, IEEE Trans. NS-23 (1976) 234.
[5] F.S. Goulding, Nucl. Instr. and Meth. 43 (1966) 1.